ELSEVIER

NeuroImage

www.elsevier.com/locate/ynimg
NeuroImage 39 (2008) 1926–1937

Regionally-specific adaptation dynamics in human object areas

Sharon Gilaie-Dotan, Yuval Nir, and Rafael Malach*

Department of Neurobiology, Weizmann Institute of Science, Rehovot, 76100, Israel

Received 24 July 2007; revised 10 October 2007; accepted 15 October 2007
Available online 22 October 2007

Functional magnetic resonance adaptation (fMR-A, also termed repetition suppression) is a reduction in activity due to repeated image presentations which has been extensively studied in human visual areas. Here we tested whether fMR-A dynamics during sustained image presentations is determined by cortical region or by stimulus category. Nine subjects were scanned while viewing a long sustained presentation of a single face or a house image. Attentional level was maintained throughout the presentation by a demanding contrast detection task. Our results show a clear regional differentiation in adaptation dynamics within high-level visual cortex—especially in the ventral stream. Face-selective regions showed an initial adaptation effect followed by a sustained level of activity for both face and house images. In contrast, activity in house-related regions showed a faster initial decline for houses, which reached essentially to baseline for the non-optimal, face images. The object-related lateral occipital (LO) region exhibited an adaptation profile similar to the face-selective regions. Importantly, within each region, the rate of signal decline from the peak activation was independent of the viewed category (preferred or non-preferred), and this was true for parietal and frontal regions as well. Thus, our results demonstrate that the functional differentiation in ventral stream regions is evident not only in their functional selectivity but also in their adaptation dynamics. Our results suggest regional rather than stimulus specificity with regard to cortical computations. These results demonstrate that the adaptation effect can in fact be compatible with models positing a tight correlation between activity levels and perceptual states.

Introduction

A number of fMRI studies have demonstrated the object-selective nature of high-order visual object areas, particularly in the ventral stream (Grill-Spector and Malach, 2004). Thus, it has been repeatedly demonstrated that certain object categories such as faces (Kanwisher et al., 1997), places (Aguirre et al., 1998; Epstein and Kanwisher, 1998), and common objects (Malach et al., 1995) elicit preferential activation in specific regions within high-order cortex when measured with fMRI (Hasson et al., 2003). A fundamental issue that is still unresolved is whether the selectivity to different object categories found in the different object areas reflects a regionally specific computational strategy applied equally to different stimuli, or alternatively, is related to stimulus-specific computations which may be preferentially associated with certain object images. For example, one could envision that a similar computational process, such as template (Lerner et al., 2002), or fragment-matching (Ullman et al., 2002), is applied throughout the entire ventral stream – with different templates being clustered in different regions – e.g. face templates in the fusiform face area (FFA) and house templates in the parahippocampal place area (PPA). Alternatively, it could be that a different computation is performed in the different areas. For example, we proposed that in the FFA, an important dimension of the computation may be analysis of fine detail, while in the PPA the complementary processes emphasize large scale integration of information (Hasson et al., 2003; Levy et al., 2001, 2004). In this case, the category selectivity observed in these regions stems from the fact that different object categories may invoke such computations to a different degree.

Here we attempted to address this issue by studying the temporal dynamics of the response through the adaptation paradigm. The adaptation effect (also termed repetition suppression (Grill-Spector et al., 2006)), in which repeated presentation of the same visual stimulus leads to reduced activation, has been studied extensively using fMRI (Grill-Spector and Malach, 2001; Krekelberg et al., 2005; Sawamura et al., 2005; Shmuelof and Zohary, 2005; Vuilleumier et al., 2005; Dehaene-Lambertz et al., 2006; Gottfried et al., 2006; Klein et al., 2006; Krekelberg et al., 2006; Yi et al., 2006; Li Hegner et al., 2007). It has proven particularly effective as an incisive tool for the analysis of neuronal properties below the conventional fMRI resolution (Grill-Spector et al., 1999; Huk et al., 2001; Kourtzi and Kanwisher, 2001; Avidan et al., 2002a; Schiltz and Rossion, 2006; Yi et al., 2006; Gilaie-Dotan and Malach, 2007; Li Hegner et al., 2007; McKyton and Zohary, 2007).

Here we adopted this approach as a tool for tapping into the computational processes in high-order object areas. We attempted to achieve this goal by driving the adaptation effect "to its limits" using a sustained presentation of 21 s of a single object image. Our results show that when adaptation effects are pushed to their extreme level, the adaptation dynamics becomes clearly differ-

* Corresponding author. Fax: +972 8 934 4131.
E-mail address: rafi.malach@weizmann.ac.il (R. Malach).
Available online on ScienceDirect (www.sciencedirect.com).

1053-8119/$ - see front matter © 2007 Elsevier Inc. All rights reserved.
doi:10.1016/j.neuroimage.2007.10.010

entiated across different object areas. In particular, the FFA and PPA showed a significantly different dynamics. Importantly, the adaptation dynamics was regionally-specific but invariant to the object category being viewed, so that within a specific region, even object images which were sub-optimal for that specific region showed adaptation dynamics similar to the optimal images. Our results support the notion that different object areas implement different computations. These computations are applied in a regionally specific manner to different object categories.

Our experiment is also relevant to more general issues concerning the relationship between neuronal activity and perception. An attractive model of visual perception posits that activity in ventral cortex may be directly correlated to the subjects' perceptual states (Grill-Spector et al., 2000; Hasson et al., 2001; Avidan et al., 2002b; Gilaie-Dotan et al., 2002). Given this notion, the adaptation effect may pose a challenge to such models in that it reveals a change in activity associated with presumably similar stimulus-driven perceptual states. Our experimental design offered a stringer test of such models since the long sustained stimulus presentation produced maximal adaptation, while maintaining the perceptual state at a fairly constant level. Our results, particularly derived from the FFA and LO, demonstrate that even under such extreme adaptation conditions, activity-related models of perception are still tenable.

Methods

Subjects

Nine healthy subjects (five women, ages 21–46, mean age 29.3 years) participated in the main "sustained image" experiment as well as in a "category selectivity" experiment; eight of these subjects participated in a retinotopy mapping experiment (see details below). All subjects had normal or corrected-to-normal vision. All the fMRI subjects provided written informed consent to participate in the experiments. The Tel-Aviv Sourasky Medical Center approved the experimental protocol.

MRI setup

Subjects were scanned in a 1.5 T Signa Horizon LX 8.25 GE scanner equipped with a standard head coil. Blood oxygenation level dependent (BOLD) contrast was obtained with gradient-echo echo-planar imaging (EPI) sequence: TR = 3000 ms, TE = 55 ms, flip angle = 90°, field of view (FOV) 240 × 240 mm^2, matrix size 80 × 80. The scanned volume consisted of 17 (six subjects) or 27 (3 subjects) nearly axial slices of 4 mm thickness and 1 mm gap with an in-plane resolution of 3 × 3 mm^2, covering the occipital, temporal, and most of the frontal cortex.

A whole-brain spoiled gradient (SPGR) sequence was acquired for each subject (FOV 240 × 240 mm^2, matrix size 256 × 256, slice thickness 1.2 mm, 124 axial slices) to allow accurate cortical segmentation, reconstruction, and volume-based statistical analysis. T1-weighted high resolution anatomic images of the same orientation and thickness as the EPI slices (in-slice resolution 1.1 × 1.1 mm^2, FOV 240 × 240 mm^2, TR = 400, TE = 14) were also acquired to facilitate the incorporation of the functional data into the 3D Talairach space (Talairach and Tournoux, 1988).

"Sustained image" experiment stimuli

Stimuli were generated on a PC, projected via an LCD projector (Epson MP 7200) onto a tangent screen positioned over the subject's forehead, and viewed through a tilted mirror. The stimuli were gray scale illustrations (as depicted in Fig. 1) and included 7 different faces (3 female faces) and 7 different houses. Two additional images (1 face and 1 house) served for training prior to the scan. Stimuli were presented as 300 × 300 pixels, occupying a visual field of 12° × 12°. The fixation image was a dark gray image (R, G, B = 65) matching the background of all the stimuli. A red central fixation dot (two-by-two pixels, 0.08° × 0.08°) was superimposed on all stimuli. Low contrast images differed in contrast (−12%) for the face or house in the foreground, while their background and fixation mark were identical to those in the original images.

Sustained presentation experiment

All subjects underwent a short training session of 1 min (one face block and one house block) prior to the "sustained image" experiment scan on a different set of stimuli. The experiment lasted 630 s and included two conditions: a single face and a single house. Each condition was repeated seven times using a different face and a different house image for each block in a controlled and counterbalanced block design paradigm. Each block lasted 21 s, with interleaving 21 s fixation periods between blocks. The first and last fixation periods lasted 30 s and 33 s respectively. Each block consisted of one stimulus presented for 21 s without flicker.

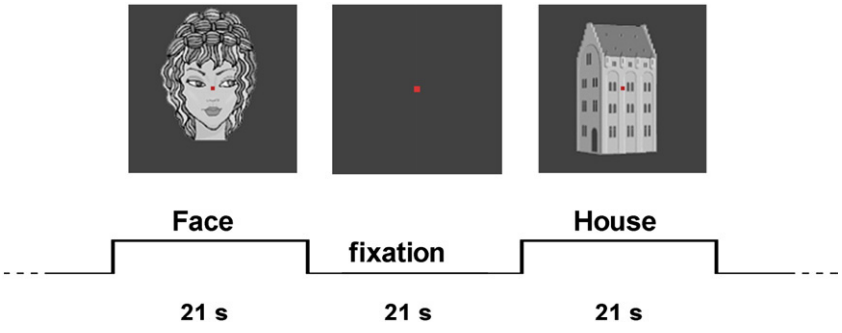

Fig. 1. Experimental design of the "sustained image" experiment. Blocks of sustained presentation of an image (face or house) lasted 21 s and were interleaved with 21 s fixation blocks. The experiment lasted 630 s and included 7 repetitions of each condition with a different stimulus in each repetition. Subjects were engaged in an attention-demanding task having to report minute contrast changes (12%) that rarely occurred.

Contrast change events of 12% attenuation (see above) lasted for 100 ms each and were rare (seven times throughout the experiment), so that only half of the blocks included such an event (4 face blocks). These events were distributed evenly along the time line of the 21 s block. Subjects' task was to fixate and report every time a contrast change was detected via a response box (Fig. 2 and Supplementary Fig. 1).

Mapping borders of retinotopic and object-selective visual areas

Eight of the nine subjects underwent an additional fMRI experiment to delineate the borders of retinotopic regions (Levy et al., 2004; see also DeYoe et al., 1994; Sereno et al., 1994; Engel et al., 1997). All subjects underwent an additional fMRI experiment to delineate the borders of category-selective regions within high-order visual cortex (category-localizer experiment described in Levy et al., 2001; experiment 1A; Fig. 3 displays a multi-subject analysis for orientation purposes). Briefly, the category-localizer experiment followed a block design paradigm, consisting of 4 conditions (faces, houses, objects, or patterns). A block consisted of nine line drawing images (of 12°×12° visual angle) of the same category, each displayed for 800 ms followed by a 200 ms blank screen. Each block lasted 9 s followed by a 6 s blank screen. Each condition (category) was repeated seven times in a pseudo-random order. The experiment lasted 450 s. The Subject's task was a covert 1-back, same–different, memory task. To that end, each block contained one or two consecutive image repetitions.

ROI definitions

V1 regions of interest (ROIs) were determined for each subject separately based on the retinotopic mapping experiment (Levy et al., 2004). Category-selective ROIs (face, house, object) were determined for each subject separately according to the category-localizer experiment (experiment 1A; Levy et al., 2001). Individual subject data from the category-localizer experiment (Levy et al., 2001; Hasson et al., 2003) were fitted to a General Linear Model (*BrainVoyager* software package (R. Goebel, Brain Innovation, Maastricht, The Netherlands)). Regions anterior to the subject's retinotopic borders that exhibited selective activations in response to a specific category (e.g. face>house and object, $p<0.05$) and that occupied at least six contiguous functional voxels were defined as category-selective ROIs. FFA ROIs were defined as face-selective regions within the posterior aspect of the fusiform gyrus. Occipital face area (OFA) ROIs were defined as face-selective regions residing in the lateral–occipital aspect of the cortex in the vicinity of the inferior occipital sulcus or gyrus (IOS or IOG respectively). PPA ROIs were defined as house-selective regions residing in the parahippocampal gyrus or the adjacent collateral sulcus. Dorsal transverse occipital sulcus (TOS) house-related ROIs (Hasson et al., 2003; Levy et al., 2004) were defined as house-selective regions in the occipito-parietal aspect of the cortex beyond retinotopic cortex in the vicinity of the transverse occipital sulcus. LO ROIs were defined as object-selective regions in the lateral–occipital aspect of the cortex in the vicinity of the inferior occipital sulcus or gyrus (IOS or IOG respectively). For the one subject that did participate in the retinotopic mapping experiment, the category-localizer experiment (Levy et al., 2001; experiment 1A) was used to delineate the category-selective regions beyond assumed retinotopic areas (showing preference to textures over objects). For this subject V1 ROIs were defined anatomically as the activated regions within the calcarine sulcus. Additional ROIs (numbered 3 to 8 in Fig. 3, and see also Fig. 6, Supplementary Fig. 3) were determined for each subject separately based on above-baseline visual activation in conjunction with anatomical location.

Peak FFA and PPA voxels were defined for each subject as the most significant voxel in the statistical test that was used to define FFA and PPA ROIs in the category-localizer experiment. These voxels were then used, in each subject, as the "peak ROI" for sampling time courses in the "sustained image" experiment.

fMRI data analysis

fMRI data were analyzed with the *BrainVoyager* software package (R. Goebel, Brain Innovation, Maastricht, The Netherlands) and with complementary in-house software. The first two images of each functional scan were discarded. The functional images were superimposed on 2D anatomical images and incorporated into the 3D data sets through trilinear interpolation. The complete data set was transformed into Talairach space

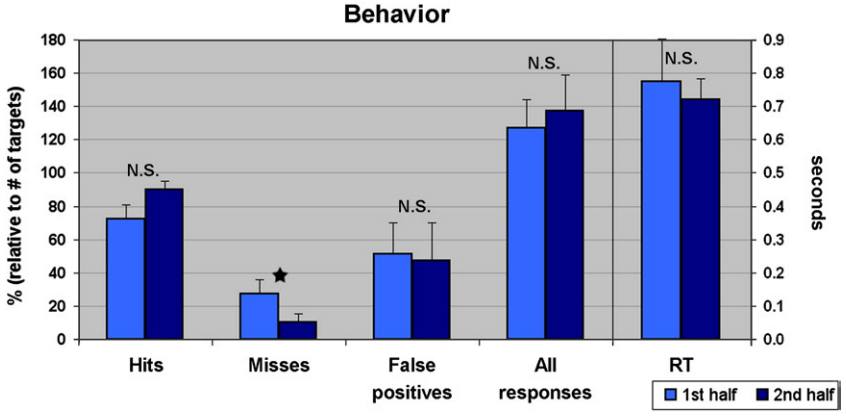

Fig. 2. Behavioral performance during the "sustained image" fMRI experiment: first versus second half of each block. Left to right: percent of hits, misses, false positives, and overall responses (relative to the number of targets), and reaction times. All performance measurements indicate that the subjects were attentive throughout the blocks. Essentially no significant difference between the first and second half of the blocks was found (see Results for more details). Error bars denote SEM between subjects ($n=9$).

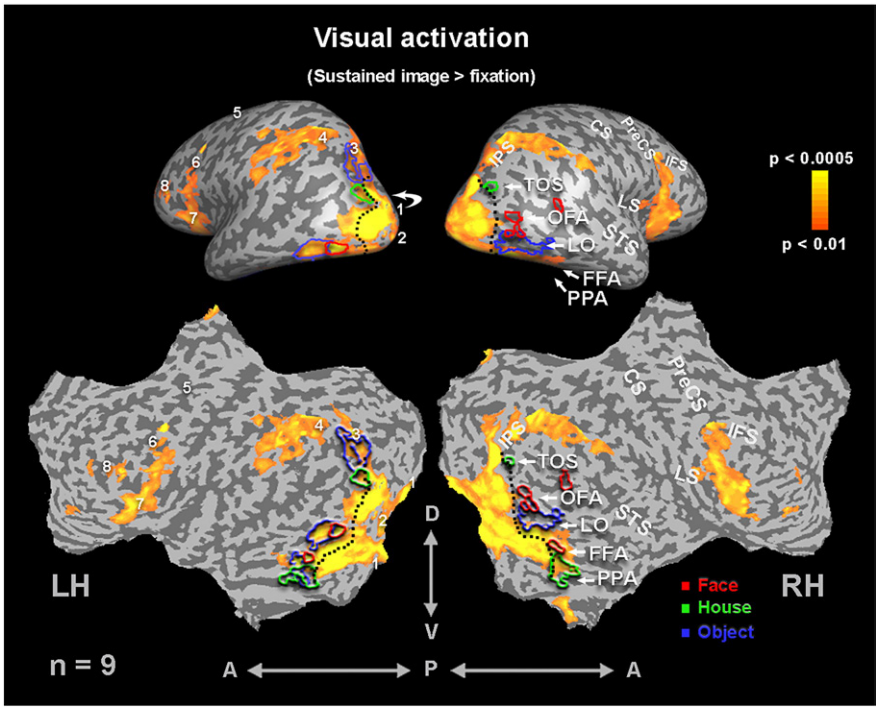

Fig. 3. Visual activation maps of the "sustained image" experiment and anatomical indications. Multi-subject data are presented both in inflated hemisphere format (top, posterior view) and in unfolded cortical format (bottom). Yellow to orange represent regions that were visually active in response to the sustained presentation of the face or house images over the fixation baseline (all conditions > fixation, $p < 0.01$, random effect, corrected, $n = 9$). Black dotted line represents the approximate anterior retinotopic border. Category-selective regions are indicated by colored lines (red, face; green, house; blue, object). Anatomical abbreviations: LH—left hemisphere, RH—right hemisphere, D—dorsal, V—ventral, P—posterior, A—anterior, PPA—parahippocampal place area, FFA—fusiform face area, LO—lateral occipital, OFA—occipital face area, TOS—transverse occipital sulcus, STS—superior temporal sulcus, IPS—intraparietal sulcus, LS—lateral sulcus (insula), CS—central sulcus, PreCS—precentral sulcus, IFS—inferior frontal sulcus. ROIs are numbered according to the following scheme: 1—peripheral V1, 2—central V1, 3—posterior IPS, 4—inferior IPS, 5—PreCS and superior frontal sulcus (SFS) intersection, 6—PreCS and inferior frontal sulcus (IFS) intersection, 7—anterior LS, 8—IFS. For display purposes only, anatomical labels are presented on the right hemisphere and the ROI enumeration on the left. $n = 9$ subjects.

(Talairach and Tournoux, 1988). Preprocessing of functional scans included 3D motion correction, slice scan time correction, linear trend removal, and filtering out of low frequencies up to 4 cycles per experiment (below 0.0064 Hz). No spatial smoothing was applied to the data.

Category-related regions were identified in each subject separately using the category-localizer experiments as described above. We then sampled the time course of activity during the sustained presentation experiment in each of the ROIs and computed the blood oxygenation level dependent (BOLD) percent signal change compared to the fixation period preceding it. We then averaged these responses across repetitions for each condition for each time point along the block. Finally, the responses were averaged across subjects for each ROI and for each condition (Figs. 4A, B and 5, Supplementary Fig. 3).

Normalized time courses of the FFA and PPA (presented in Figs. 4C, D) were calculated for each subject relative to the peak response to the region's preferred category which occurred 6 s after stimulus onset (indicated by the beginning of the gray zone in Fig. 4). Normalization was applied so that each time point along the time course was calculated as percentage of the maximal peak response to the preferred category. Normalized time courses in the other ROIs were calculated according to the same time point (6 s after stimulus onset), so that the dynamics could be compared across regions for the same point in time.

Structural MRI data analysis

The cortical surface was reconstructed from the 3D SPGR scan. The procedure included segmentation of the white matter using a grow-region function, the smooth covering of a sphere around the segmented region, and the expansion of the reconstructed white matter into the gray matter. The surface of each hemisphere was then unfolded, cut along the calcarine sulcus and additional predefined anatomical landmarks on the medial side, and flattened.

Adaptation dynamics indices (ADI, maxADI) and minimum MR signal

The adaptation dynamics index (ADI, percent drop per second, Fig. 6) was calculated as

$$\begin{aligned}\mathrm{ADI} &= \%\ \text{change from } T_{\mathrm{peak}}/\mathrm{s} \\ &= \frac{(\mathrm{normSignal}_{T_{\mathrm{peak}+6\ \mathrm{s}}} - \mathrm{normSignal}_{T_{\mathrm{peak}}})}{6},\end{aligned}$$

where T_{peak} denotes the time point 6 s after stimulus onset (peak activation in the FFA and PPA), and $T_{\mathrm{peak}+6\ \mathrm{s}}$ denotes the time point 6 s after T_{peak}. This was calculated for each subject and each category and then averaged across subjects.

A minimum in the MR signal relative to the subjects' peak response (calculation restricted to 3 to 24 s after stimulus onset)

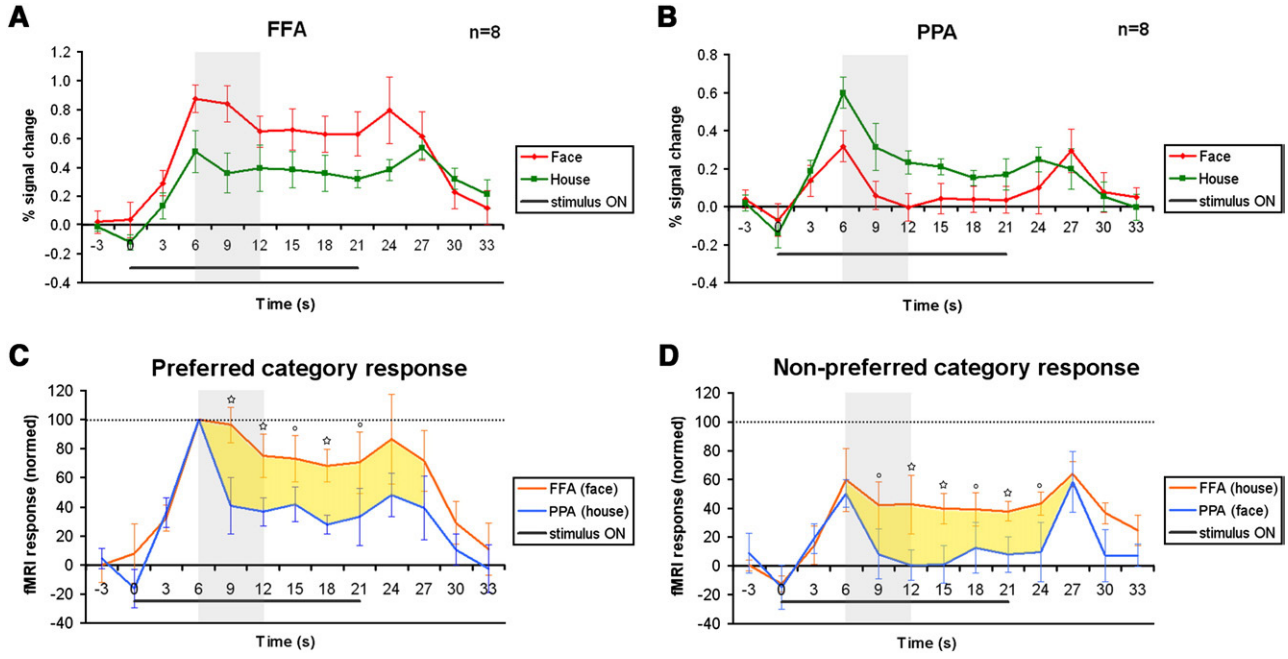

Fig. 4. FFA and PPA adaptation time courses. (A) FFA average time course to preferred face images (red) and non-preferred house images (green) during sustained image presentation. (B) PPA average time course to preferred house images (green) and non-preferred face images (red). Black line below the *x*-axis indicates when the stimulus was on. (C, D) Normalized time courses to preferred (C) and non-preferred (D) categories relative to the peak response of each region to its preferred category. Dashed black line (100%) indicates the peak response to the preferred category. FFA's response is displayed in orange, PPA's response is in blue. The yellow area indicates the difference between the FFA's and PPA's responses to their preferred (C) and non-preferred (D) categories (faces and houses respectively) throughout the sustained presentation. Black asterisks indicate significant difference ($p<0.05$, 1-tailed equal variance *t*-test, $n=8$) between the responses of the FFA and the PPA at specific time points, black circles indicate a nearly significant difference ($0.05 \le p \le 0.10$). Gray region indicates the time window of the major adaptation in the FFA and PPA for both categories (this time window was used to calculate the ADI, see Results and Methods). Note that the PPA's response profile (B) is more transient while the FFA (A) has an initial decline and then maintains sustained activity throughout the block. This is true for both the preferred (C) and non-preferred (D) categories. Error bars denote SEM between subjects.

was found for each subject for each of the categories in both the FFA and the PPA and then averaged across subjects.

The maximum ADI (maxADI) was calculated in a similar manner as the ADI. The time period taken to calculate the percent drop per second was now determined for each subject specifically from the subjects' maximum until the subjects' minimum response during the block (as opposed to a fixed 6 s time zone for the ADI calculation).

Multi-subject analysis

To obtain the multi-subject maps presented in Fig. 3, the time courses of all subjects were converted into Talairach space and *z*-normalized. The "sustained image" visual activation map was obtained by contrasting activations to face and house images over fixation baseline ($p<0.01$, random effect, corrected, $n=9$). Statistical significance levels were calculated taking into account the individual voxel significance, a minimum cluster size of 9 functional voxels, and the probability threshold of a false detection of any given cluster within the entire cortical surface (Forman et al., 1995). This was achieved using a Monte Carlo simulation (AlphaSim by B. Douglas Ward, a software module in Cox (1996)). The category-selective maps were obtained by contrasting activation to one category with the activation to the other categories (e.g. face-selective by (face>house, object), $p<0.05$, fixed effect, $n=9$). For visualization purposes the maps were projected on a flattened Talairach normalized brain.

Behavioral data

Responses were collected during the fMRI "sustained image" experiment via a response box. Responses were considered as related to contrast change events if they occurred within 4000 ms after these events (otherwise they were treated as false positives). Reaction time (RT) and error rate data were collected for each scan. Additional analysis of the behavior by the first half (10.5 s) and second half (10.5 s) of each block was also done to control for maintained attention along the block and to verify that the behavior of the subjects did not wane. This was done for each subject separately and then averaged across subjects.

Results

Our aim in this study was to uncover potential differences in the adaptation dynamics which might vary across different object-related visual regions and within a region depending on the specific stimulus category being processed. To that end, we constructed an experiment in which the adaptation effect was driven to its maximum level. The "sustained image" experiment was designed to accomplish this goal. In the experiment the subjects viewed long

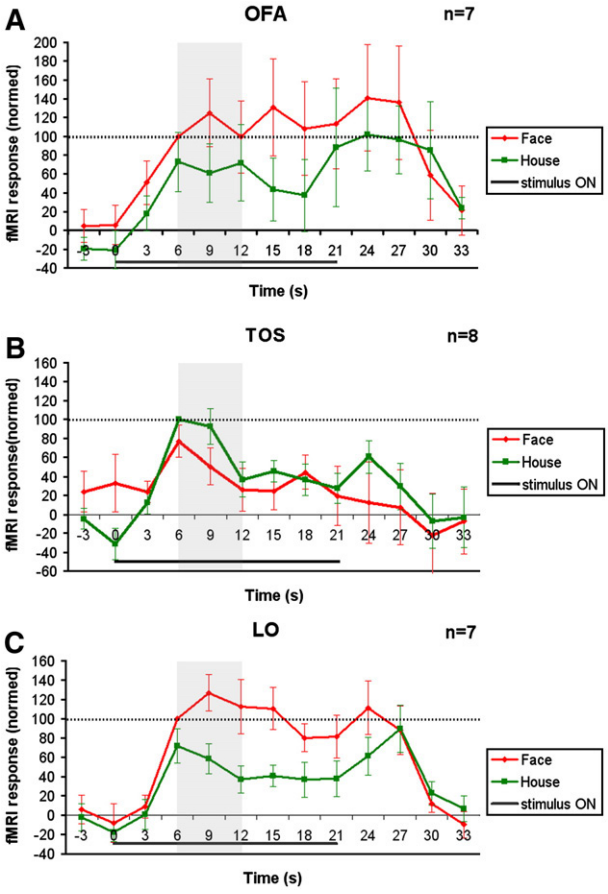

Fig. 5. Time courses of dorsal ventro-occipital cortex, category-selective regions. Average time courses of "mirror" category-selective dorsal occipito-temporal regions and LO (see Results). Same display format as Fig. 4. Note that the adaptation dynamics in OFA (A) and LO (C) seems to resemble that observed in the FFA (Fig. 4A), whereas the dynamics in TOS (B) seems more similar to that found in the PPA (Fig. 4B). Error bars denote SEM between subjects.

(21 s) sustained presentations of either a single face or a single house (Fig. 1). During the presentation, subjects were engaged in a demanding contrast detection task. The task was designed to keep the subjects continuously attentive to the stimuli throughout the long constant presentation of each stimulus (see Methods for more details).

As depicted in Fig. 2, behavioral measures including RT and error rate revealed that the subjects were attentive to the stimuli at a fairly constant level throughout the experiment. A quantitative analysis revealed no difference in performance between the first and second halves of each block (false positives $p>0.35$, number of responses $p>0.33$, RT $p>0.33$). Moreover, there were even fewer misses in the second half ($p<0.05$, paired one-tailed t-test for first vs. second half). Similarly, the performance on the face and house images was similar (RT: $p>0.12$, paired two-tailed t-test; number of responses: $p>0.38$, paired two-tailed t-test, and see also Supplementary Fig. 1).

Despite the fact that only a single image was presented in each block, the visual activation was consistent and robust as can be seen in Fig. 3 which displays the visual activation in response to either a face or a house image relative to the fixation baseline.

Adaptation dynamics in ventral regions: FFA and PPA

Since both the FFA and the PPA are well documented in the literature with respect to their preferred and non-preferred categories (Kanwisher et al., 1997; Aguirre et al., 1998; Epstein and Kanwisher, 1998; Ishai et al., 1999; Tong et al., 2000; Hasson et al., 2003), the adaptation dynamics in these regions was our primary interest since the dependence of the adaptation on category preference could be easily examined. We identified the face-selective FFA and house-selective PPA for each subject using a separate "localizer" experiment (see details in Methods). The "sustained image" experiment time courses were then sampled from these ROIs and analyzed. Fig. 4 displays the FFA's (panel A) and PPA's (panel B) average time courses in response to face (red) and house stimuli (green). Comparing these time courses revealed a difference *between* the regions in their adaptation dynamics while *within* each region the adaptation dynamics was similar for both object categories—albeit with a higher amplitude to the preferred category (see the shape of the response within a region for both categories). A similar difference in inter-areal dynamics was also found when the sampling was restricted to peak voxels (see Supplementary Fig. 2).

In order to quantify this difference between the regions and to allow for a direct comparisons between them, we transformed the percent signal change (PSC) values of each region to common

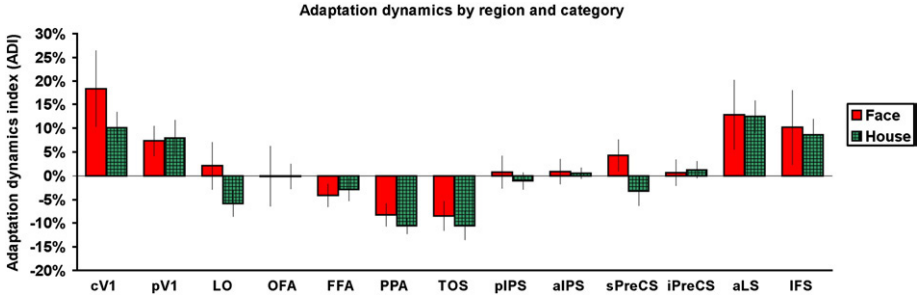

Fig. 6. Adaptation dynamics by regions and category. Adaptation dynamics indices (ADI) were calculated for each category in each ROI. These indices indicate the average rate of adaptation in the critical time window when the major reduction in the FFA and PPA took place (see gray regions in Figs. 4, 5 and Supplementary Fig. 3). ADI for houses indicated in green, for faces in red. Notably, only a significant effect of *region* was found, without any effect of category or interaction between them (see Results for details). Moreover, an explicit examination for each region confirmed that within each region there was no significant difference between the face and house adaptation indices (1-tailed paired t-test, $p>0.11$). Error bars denote SEM between subjects.

normalized values (as displayed in Figs. 4C, D by category preference, see Methods for details).

First, for each region and each category we examined whether there was a significant adaptation effect, when did it occur in time, and what was its extent. To that end we ran a two-way ANOVA (category (face, house) and time point (12 points along block from stimulus onset), $n=8$) looking for time point effects after the peak activity, which would indicate adaptation.

For the FFA this analysis yielded a significant effect for time point ($p<0.0001$), and an expected effect of category ($p<0.002$) which reflected the amplitude bias for the preferred category. In order to determine whether the effect we found for time point indicated a significant adaptation, we compared (Fisher's PLSD post hoc analysis) the initial transient peak response with the responses at time points following the peak. We found that after 6 s there was a nearly significant adaptation effect in the FFA ($p<0.08$), and it reached significance 12 s after the peak response ($p<0.031$), dropping to 68%±11% (SEM) of the maximal response to faces, and to 66%±19% (SEM) of the maximal response to houses. Additional analysis confirmed that throughout the block the response of the FFA was significantly different from baseline for both the preferred and non-preferred categories ($p<0.035$ for all time points). This indicates that the FFA maintained a substantially sustained activity level throughout the block regardless of the viewed category.

The same analysis revealed a different dynamics for the PPA. Here also, a time point effect that could indicate adaptation was found ($p<0.0001$), as well as an effect for category ($p<0.02$) — reflecting an amplitude response bias. However, the adaptation effect here was much faster compared to that found in the FFA, reaching significance immediately following the peak activation (3 s, $p<0.001$), and its magnitude was already greater at that point than the FFA's adaptation after 12 s (PPA dropping to an average of 41%±21% (SEM) of the maximal response to houses and to an average of 17%±34% (SEM) of the maximal response to faces). We also found that the PPA's response was maintained above baseline throughout the block only for its preferred category ($p<0.04$ until and including 24 s after stimulus onset), while for its non-preferred category the response was not significantly different from baseline during most of the block following the initial transient ($p>0.23$, with the exception of a probable post-stimulus rebound effect—27 s after stimulus onset, $p<0.02$). These results suggest a much more transient processing mechanism in the PPA regardless of the processed category.

Given the foveal bias of the FFA (Levy et al., 2001; Hasson et al., 2003), it was important to rule out the possibility that the sustained response of the FFA was due to small eye movements. To that end, we sampled the activity from both central and peripheral V1. If eye movements were a dominant factor in the FFA's sustained activity, we would expect to see a more sustained response in central vs. peripheral field locations in area V1. The sampled time courses are displayed in Supplementary Fig. 3. A direct comparison between central V1 and peripheral V1 along the time line did not reveal a significant difference in adaptation dynamics (three-way ANOVA results for region $p>0.75$, $F<0.11$; for category $p>0.34$, $F<1$; for time point $p<0.0001$, $F>25$; no two-way interactions with respect to region were found). Therefore, it is unlikely that the small fixational eye movements may have underlain the sustained FFA activity.

In order to obtain a more quantitative estimate of the adaptation dynamics in the FFA and the PPA we calculated for each category an adaptation dynamics index (ADI). The ADI indicated the rate of signal decline from its peak response within 6 s after the peak (as indicated by the gray zone in Fig. 4 panels; see detailed procedure and application to other ROIs in Methods). A negative value of this index indicates adaptation, a positive value indicates an activation enhancement, and zero indicates on sustained activity.

For the FFA the ADI was found to be −4.1±2.5 (SEM) for faces and −2.8±2.5 (SEM) for houses, whereas the PPA manifested significantly more negative values corresponding to faster and more profound adaptation (−8.3±2.5 (SEM) for faces, and −10.6±1.7 (SEM) for houses). A two-way ANOVA on these ADI values revealed that the adaptation was determined only by cortical region and not by category (region effect: $p<0.012$, $F>7.3$; no category effect: $p>0.81$, $F<0.06$; no interaction: $p>0.42$, $F<0.7$).

To obtain an additional quantitative measure of the response dynamics we also calculated the MR minima along the response time course (see Methods). The time of the MR minima in the FFA showed substantial inter-subject variability (occurred at an average time of 14.3 s±6.8 s (SD) after the peak for faces, and at an average time of 9.8 s±5.5 s (SD) for houses). The decline in signal in the FFA was 43%±16% (SEM) from the maximum MR signal for faces and to 23%±12% (SEM) of the maximum MR signal to houses. In the PPA, the minima MR signal occurred at an average time of 12 s±7.2 s (SD) after the peak for houses and at an average time of 9.0 s±5.1 s (SD) for faces, reaching a minimum value of −1%±6% (SEM) from the peak response to houses and −90%±53% from the peak response to faces.

The rate of signal decline from the maxima to these minima was calculated as the maximum ADI (maxADI, see Methods for details). The maxADI values in the FFA were found to be −5.1±0.7 (SEM) for faces, −11.7±3.9 (SEM) for houses. In the PPA for houses −17.4±5.2 (SEM) and for faces −51.4±20.3 (SEM). A two-way ANOVA on these maxADI values again indicated that the adaptation dynamics was determined by region ($p<0.03$, $F>6$), not determined by category ($p>0.2$, $F=1.68$), and interaction between region and category did not reach significance ($p=0.065$, $F=3.96$).

We also examined the potential differences in dynamics between the FFA and the PPA when the emphasis was on the categorical preference dimension.

Fig. 4C shows the response of these regions to their *preferred* category. To verify the significance of the difference between these two regions in their response to their preferred category – which is clearly evident in Fig. 4C (colored in yellow) – we ran a statistical analysis (two-way ANOVA for region and time point, examining the regions' responses to their preferred category along time (from the peak activation)). The result of this analysis revealed a significant effect for region ($p<0.0001$, $F>18$) and a significant effect for time point ($p<0.02$, $F>2.7$) with no interaction ($p>0.65$, $F<0.65$). When we confined the time variable to the time window used to calculate the ADI (gray regions in Fig. 4) we found an almost significant interaction between region and time point which most probably reflected the more rapid adaptation in the PPA than in the FFA (region: $p<0.002$, $F>11$; time point: $p<0.002$, $F>7$, interaction: $p=0.0572$, $F=3.065$). We further analyzed the difference between the regions' responses along time, checking the significance of this difference for each time point along the block (indicated by asterisks ($p<0.05$, 1-tailed equal variance t-test, $n=8$) and black circles ($0.05\leq p\leq 0.10$) in Fig. 4C). This analysis revealed that along most of the response there was a significant

difference between these regions' responses to their preferred categories, although at some time points this difference was only close to significance (see time points indicated by dots in Fig. 4C). Importantly, in the major adaptation time window (time points within 6 s after the peak) the response to the preferred category was significantly different.

An identical analysis of the responses of the FFA and PPA to their *non-preferred* categories was performed and is presented in Fig. 4D. Again, we found a significant effect for region ($p=0.0001$, $F>15$), no effect for time point ($p>0.22$, $F=1.4$), and no interaction ($p>0.94$, $F<0.3$).

So both for preferred and for non-preferred stimuli, we found a significant regional difference, again with the FFA keeping a more sustained elevated response than the PPA.

Adaptation dynamics in dorsal regions

In previous studies we proposed that the FFA and PPA have "mirror" regions located dorsally, which share similar functional properties associated with their central/peripheral visual field bias (Malach et al., 2002; Hasson et al., 2003). Thus, it was of interest to compare the adaptation profiles in these regions to those of the FFA and PPA. These areas, including the occipital face area (OFA) and the dorsal house-related transverse occipital sulcus (TOS) (Hasson et al., 2003; Levy et al., 2004; Epstein et al., 2007), were also identified for each subject using a separate "localizer" experiment (see details in Methods). The time courses obtained from these regions are depicted in Figs. 5A and B. Similar to their object selectivity profile, the adaptation dynamics of these two regions appeared to mimic those of the FFA and PPA. The face-selective OFA manifested sustained above-baseline activity for both faces and houses throughout most of the block (faces: $p<0.05$ for all time points, houses: nearly significant with $p<0.07$ for all but 2 time points, 1-tailed t-test). Moreover, the reduction rates were similar to those found in the FFA (keeping a level of 99% ±39% (SEM) of the response to faces within the equivalent time window, 99%±56% (SEM) for houses). The house-selective TOS region, on the other hand, displayed a sharp reduction in the activity following the peak response (dropping to 37%±18% (SEM) of the response to houses, and to 34%±29% (SEM) of the maximal response to faces), similar to the PPA. Importantly, as can be seen in the figure, although these regions' time courses were noisier—both regions appeared to display similar dynamics to both preferred and non-preferred categories, as was seen in the FFA and the PPA.

Adaptation and enhancement dynamics in other regions

As depicted in Fig. 3 the face and house images elicited a widely distributed activity in additional cortical areas—including the object-selective LO (Hasson et al., 2003), early visual areas, parietal, and prefrontal regions. It was of interest to examine the activity profiles in these additional regions in response to the sustained presentation. We defined the LO object-selective region in the lateral–occipital aspect of the cortex using a separate "localizer" experiment (objects > faces and houses, see Methods). We found that its overall activity profile (see Fig. 5C) was similar to that found in the FFA, both in terms of having fairly sustained activity along time from the activation level 6 s after stimulus onset ($p>0.12$ for all time points, post hoc Fisher's PLSD), and in terms of its ADI values which differed significantly from the PPAs (post hoc Fisher's PLSD $p<0.05$), but not from the FFAs ($p>0.66$). Here again, there was no significant difference observed between the adaptation dynamics to the face and house stimuli ($p>0.11$).

It was of interest to examine whether the adaptation was a global phenomenon in all visually responsive cortical areas. To that end we also examined additional visual regions (early visual cortex: peripheral V1, indicated as region 1 in Fig. 3 ROI list, and central V1, region 2 in Fig. 3; intraparietal sulcus (IPS) regions: posterior IPS (3) and anterior IPS (4)), as well as prefrontal regions along the precentral sulcus (regions 5 and 6 in Fig. 3), anterior lateral sulcus (region 7), and inferior frontal sulcus (region 8). These regions were identified by a conjunction of significant visual activation and anatomical location (for V1 the definition was based on the retinotopic maps of each subject as well). It was also of interest to examine whether these additional regions would show a category-dependent differentiation in the response dynamics.

We sampled the time courses of all these regions (see Supplementary Fig. 3) and then calculated the adaptation dynamics index (ADI) as was done for the FFA and PPA (see Methods for details). The indices for each region and each category are depicted in Fig. 6. A two-way ANOVA (ROI and category) on the index values of all the regions revealed that the response change depended only on the region and not on the category being processed (region effect: $p<0.0001$, $F>8.4$; no effect for category: $p>0.13$, $F>2.2$; no interaction: $p>0.95$, $F<0.42$). Post hoc analysis confirmed that there was no significant difference between the "mirror" ventral and dorsal regions (FFA vs. OFA: $p>0.36$, PPA vs. TOS: $p>0.98$). V1 exhibited a sluggish buildup followed by slow continuous adaptation that was reflected in positive ADI values (Supplementary Figs. 3A and B). In contrast, frontal regions showed an opposite trend of a continuous buildup of activity as the stimulation progressed (Supplementary Figs. 3F and H).

Additional dynamics

Interestingly, in some of the regions we examined, we found a post-stimulus rebound effect, i.e. an increase in the response once the stimulus was turned off. These regions included category-related regions such as the FFA, PPA, LO, and TOS, but surprisingly did not include V1 regions (see Supplementary Fig. 3). In the FFA and PPA the effect was more pronounced for the non-optimal category, although it was also observed for the preferred category but to a lower extent. It is also likely that the slight enhancement in activity for houses in IFS and aLS that appeared once the stimulus was turned off was related to the same phenomenon.

Discussion

Adaptation dynamics determined by regional mechanisms

We found that the adaptation parameters such as decline rate and magnitude were determined by regionally specific mechanisms, and were *independent* of the object category being viewed. Thus, for each region, similar dynamics was observed both for the optimal stimuli (faces in the FFA and houses in the PPA, Fig. 4C) and for the non-optimal stimuli (Fig. 4D). This was also true for regions which did not display strong category selectivity (see Fig. 6 and Supplementary Fig. 3). Thus, the profile of adaptation dynamics was region-specific rather than category-specific. These findings are compatible with our previous report showing

category-invariant adaptation effects in ventral stream areas (Avidan et al., 2002a). These results are also in line with the proposal that different neuronal mechanisms could underlie fMRI adaptation (Grill-Spector et al., 2006). Here we report that the regional adaptation dynamics relies on specific regional properties and these may be explained by some of the suggested models in Grill-Spector et al. (2006). Concerning the dynamics we observed in visual areas outside the FFA and PPA, such as early visual cortex and LO, it should be noted that the stimuli used in the present experiment may not have been the optimal ones for these areas. Although the results concerning the FFA and PPA illustrate a similar dynamics for both optimal and non-optimal stimuli, the situation may be different in other areas. For example, in area V1 we may observe a different dynamics for more low level stimuli compared to the face and house images used here.

An alternative interpretation for the category invariance of the adaptation we found in each region is that it may have been due to a very broad category tuning curve of the underlying neuronal population. Thus, it could be argued, for example, that the same FFA neurons which were optimally tuned to face images also responded, albeit at a weaker level, to house images and thus showed a similar adaptation profile.

However, recent studies using fMR adaptation demonstrated that such a broad tuning model is unlikely, and in fact adaptation effects in the FFA show even a sub-exemplar tuning specificity (Gilaie-Dotan and Malach, 2007). Furthermore, we have found previously that reduced single neurons' responses resulting from sub-optimal stimuli, such as low contrast images, produce a weaker adaptation effect compared to optimal stimuli—regardless of the overall fMRI signal level (Avidan et al., 2002a). Such a reduction in adaptation level was not observed here for the non-optimal category stimuli, suggesting that they likely reflect an optimal response of small islands of neurons within the overall population (cf. adaptation dynamics of optimal to non-optimal stimuli in Figs. 4A, B). In summary, both of these sets of studies support the interpretation that the non-optimal house images in the FFA and face images in the PPA underwent a neuronal computation of a similar type as that performed for the optimal categories.

Although both FFA and PPA exhibit high category selectivity (for FFA see Puce et al., 1996; Kanwisher et al., 1997; McCarthy et al., 1997; Halgren et al., 1999; Gauthier et al., 2000; Haxby et al., 2001; for PPA see Puce et al., 1996; Aguirre et al., 1998; Epstein and Kanwisher, 1998; Halgren et al., 1999; Downing et al., 2006), we have found that their adaptation profiles were inherently different, regardless of their preferred or non-preferred responses. Their adaptation differed in its rate (PPA—rapid (3 s), FFA—mild (6–12 s)), its magnitude (FFA—mild (approximately to 67%), PPA—deep adaptation (to 41% and even less)), and even in respect to the preferred category and to the non-preferred category—likely along the full time line.

We have found that there was a unique adaptation profile to each of these regions that was independent of the processed category.

Potential confounds

The fact that similar adaptation profiles were observed regardless of object category rules out the possibility that the sustained response may have been due to a particularly strong initial response. Thus, although the initial response to house images was weaker in the FFA compared to the PPA, it nevertheless showed a more sustained response profile (cf. FFA Fig. 4A, green curve, approximately 0.51±0.14 (SEM) PSC and PPA in Fig. 4B, green curve, approximately 0.60±0.08 (SEM) PSC).

This regional difference in adaptation dynamics is relevant to the potential role of attention in the adaptation phenomena. Indeed, fMR adaptation was often attributed to attentional effects, i.e. reduced activation associated with reduced arousal or focus on the visual target. There are studies that examine this relation by varying the tasks, which are often stimulus specific, or varying the attentional demands (Murray and Wojciulik, 2004; Yi et al., 2006). The present results, particularly in the PPA, argue against the interpretation that fMR adaptation is solely due to a reduction in attention level. Thus, despite the similar tasks and attentional demands throughout the exposure duration, the PPA manifested a significantly different adaptation dynamics compared to the FFA. Thus, our results provide an apparent demonstration that adaptation dynamics may be dissociated from the levels of attention and task demands.

Finally, a possible confound may have been due to small fixational eye movements. Given the foveal bias of LO and FFA (Levy et al., 2001; Hasson et al., 2003), it could be argued that these areas may have shown higher sustained activity due to such eye movements. Two factors argue against such an interpretation. First, FFA showed a substantial positional invariance (Grill-Spector et al., 1999) which should have reduced its sensitivity to small eye movements. Furthermore, examining this issue by contrasting the activations in central vs. peripheral V1 representations (see Results and Supplementary Fig. 3 for their time courses) did not reveal a significant difference, again arguing against a role for eye movements in "refreshing" the stimulus activation in these areas.

Mirror-region dynamics

In a previous study we proposed that object-selective regions in the dorsal aspect of occipito-temporal cortex (beyond retinotopic regions) may be mirror-like duplicates of the ventral stream organization (Hasson et al., 2003). Our present results support this notion since, in dorsal and ventral occipito-temporal regions showing similar category selectivity, we now identified corresponding adaptation dynamics. It is still an open question what is the cause of these apparent duplications. We previously proposed that the basic eccentricity arrangement that extends into high-order visual cortex (Hasson et al., 2003; Levy et al., 2001, 2004; Larsson and Heeger, 2006) may underlie this pair-wise development of a dorsal and ventral set of category-related regions.

V1 and fronto-parietal areas

We found that a sustained presentation of visual stimuli elicited a widespread activation throughout the cortex extending beyond classical visual regions to parietal and prefrontal regions. The extent of the activation could be attributed to the demanding attentional tasks since it seems to overlap with fronto-parietal regions that have been reported in earlier studies as involved in various cognitively demanding tasks (Courtney et al., 1998; Lumer et al., 1998; Duncan and Owen, 2000; Rees et al., 2002; Pins and Ffytche, 2003; Sala et al., 2003; Hon et al., 2006; Gilaie-Dotan and Malach, 2007).

When examining regional adaptation dynamics (time courses and ADI) on the posterior–anterior axis (Fig. 6), the adaptation effects in V1 were sluggish, but continuous throughout the sustained period (Supplementary Fig. 3), in agreement with previous reports (Tootell et al., 1998; Grill-Spector et al., 1999). In parallel with the sluggish adaptation, the buildup of response magnitude was also sluggish (manifested as a positive ADI). The source of this dynamics is not clear—but could not be attributed simply to eye movements (see above). One possibility is that rapid transient responses in V1 activity may have been missed due to the slow hemodynamic signal of fMRI. In contrast, frontal regions showed an opposite trend, of a continuous buildup of activity along the sustained image presentation (Supplementary Fig. 3). The source of this trend might be related to high-level frontal functions such as working memory (Courtney et al., 1998; Sala et al., 2003) or priming (van Turennout et al., 2000, 2003). Parietal regions displayed near-zero ADI values indicating no change in activation levels consistent with the stable attention levels indicated by our behavior results (Mesulam, 1999; Wojciulik and Kanwisher, 1999; Kastner and Ungerleider, 2000; Behrmann et al., 2004; Husain and Nachev, 2007).

Rebound effects

An interesting phenomenon which occurred to various degrees in all ventral stream areas was a rebound effect, i.e. an increase in fMRI signal immediately following the termination of the image presentation. Several mechanisms may account for this effect, including a purely hemodynamic rebound. However, an intriguing possibility could be that this effect relates to the appearance of a negative afterimage of the sustained object during the fixation period, which some subjects reported on. Such a change in stimulus may have produced an increased activation. Interestingly, these effects were not apparent in V1, perhaps due to their relatively short duration. However, the precise cause of this effect and the parameters that determine its magnitude will require further study.

Adaptation effects and activity-based models of perception

Our study reveals that FFA, OFA, and LO showed a sustained level of activation over long exposure times (Figs. 4 and 5). Besides their relevance to a better understanding of the adaptation process, these results are of particular importance for neuronal models of perception. A number of previous studies support the notion that activity in high-order object cortex tightly corresponds to the subject's perceptual state (Tong et al., 1998; Grill-Spector et al., 2000; Hasson et al., 2001; Kourtzi and Kanwisher, 2001; Avidan et al., 2002b; Gilaie-Dotan et al., 2002; Gilaie-Dotan and Malach, 2007). From this perspective, it should be noted that previous adaptation effects appeared to pose a potential challenge to such models by revealing a consistent reduction in neuronal activity despite persistent visual stimulus (Grill-Spector and Malach, 2001). However, as already noted by James (1890), the novel perceptual state during the initial exposure to a stimulus is drastically different from that following its repeated presentation. In the present experiment we subjected the activity model to a stringer test. By extending the stimulus exposure for a long duration while maintaining the attentional demand constant, we presumably created a fairly sustained perceptual state. Under such conditions the question was—will activity in high-order object areas behave according to the perceptual state (sustained) or follow the initial adaptation dynamics (decline) (Portas et al., 2000)?

Our results indicate that activity in LO, OFA, and the FFA was compatible with a model positing a tight link between activity level and perceptual states. Thus, we propose that the sustained FFA, OFA, and LO activity may correspond to the sustained visual percepts that were not altered in spite of the long exposure durations. The initial transient may correspond under this hypothesis to the enhanced vividness associated with image novelty.

PPA and its dorsal "mirror" TOS region (Hasson et al., 2003; Levy et al., 2004) as well as V1 exhibited a different adaptation dynamics. Following the above logic regarding activity levels and sustained perception, these results may suggest a possible dissociation between PPA, TOS, and V1 activities and perceptual states.

Acknowledgments

This study was supported by the ISF Center of Excellence, the Dominique Center, and the Nella and Leon Benoziyo Center for Neurological Diseases. We thank the Wohl Institute for Advanced Imaging in the Tel Aviv Sourasky Medical Center. We thank Shani Offen for her help, Kalanit Grill-Spector for fruitful discussions, Michal Harel for brain reconstruction and flattening procedures, Eli Okon for technical assistance, and Ifat Levy for comments on the manuscript.

Appendix A. Supplementary data

Supplementary data associated with this article can be found, in the online version, at doi:10.1016/j.neuroimage.2007.10.010.

References

Aguirre, G.K., Zarahn, E., D'Esposito, M., 1998. An area within human ventral cortex sensitive to "building" stimuli: evidence and implications. Neuron 21, 373–383.

Avidan, G., Hasson, U., Hendler, T., Zohary, U., Malach, R., 2002a. Analysis of the neuronal selectivity underlying low fMRI signals. Curr. Biol. 12, 964–972.

Avidan, G., Harel, M., Hendler, T., Ben-Bashat, D., Zohary, E., Malach, R., 2002b. Contrast sensitivity in human visual areas and its relationship to object recognition. J. Neurophysiol. 87, 3102–3116.

Behrmann, M., Geng, J.J., Shomstein, S., 2004. Parietal cortex and attention. Curr. Opin. Neurobiol. 14, 212–217.

Courtney, S.M., Petit, L., Maisog, J.M., Ungerleider, L.G., Haxby, J.V., 1998. An area specialized for spatial working memory in human frontal cortex. Science 279, 1347–1351.

Cox, R.W., 1996. AFNI: software for analysis and visualization of functional magnetic resonance neuroimages. Comput. Biomed. Res. 29, 162–173.

Dehaene-Lambertz, G., Dehaene, S., Anton, J.L., Campagne, A., Ciuciu, P., Dehaene, G.P., Denghien, I., Jobert, A., Lebihan, D., Sigman, M., Pallier, C., Poline, J.B., 2006. Functional segregation of cortical language areas by sentence repetition. Hum. Brain Mapp. 27, 360–371.

DeYoe, E.A., Bandettini, P., Neitz, J., Miller, D., Winans, P., 1994. Functional magnetic resonance imaging (FMRI) of the human brain. J. Neurosci. Methods 54, 171–187.

Downing, P.E., Chan, A.W., Peelen, M.V., Dodds, C.M., Kanwisher, N., 2006. Domain specificity in visual cortex. Cereb. Cortex 16, 1453–1461.

Duncan, J., Owen, A.M., 2000. Common regions of the human frontal lobe recruited by diverse cognitive demands. Trends Neurosci. 23, 475–483.

Engel, S.A., Glover, G.H., Wandell, B.A., 1997. Retinotopic organization in human visual cortex and the spatial precision of functional MRI. Cereb. Cortex 7, 181–192.

Epstein, R., Kanwisher, N., 1998. A cortical representation of the local visual environment. Nature 392, 598–601.

Epstein, R.A., Higgins, J.S., Jablonski, K., Feiler, A.M., 2007. Visual scene processing in familiar and unfamiliar environments. J. Neurophysiol. 97, 3670–3683.

Forman, S.D., Cohen, J.D., Fitzgerald, M., Eddy, W.F., Mintun, M.A., Noll, D.C., 1995. Improved assessment of significant activation in functional magnetic-resonance-imaging (fMRI)—Use of a cluster-size threshold. Magn. Reson. Med. 33, 636–647.

Gauthier, I., Skudlarski, P., Gore, J.C., Anderson, A.W., 2000. Expertise for cars and birds recruits brain areas involved in face recognition. Nat. Neurosci. 3, 191–197.

Gilaie-Dotan, S., Malach, R., 2007. Sub-exemplar shape tuning in human face-related areas. Cereb. Cortex 17, 325–338.

Gilaie-Dotan, S., Ullman, S., Kushnir, T., Malach, R., 2002. Shape-selective stereo processing in human object-related visual areas. Hum. Brain Mapp. 15, 67–79.

Gottfried, J.A., Winston, J.S., Dolan, R.J., 2006. Dissociable codes of odor quality and odorant structure in human piriform cortex. Neuron 49, 467–479.

Grill-Spector, K., Malach, R., 2001. fMR-adaptation: a tool for studying the functional properties of human cortical neurons. Acta Psychol. (Amst) 107, 293–321.

Grill-Spector, K., Malach, R., 2004. The human visual cortex. Annu. Rev. Neurosci. 27, 649–677.

Grill-Spector, K., Kushnir, T., Edelman, S., Avidan, G., Itzchak, Y., Malach, R., 1999. Differential processing of objects under various viewing conditions in the human lateral occipital complex. Neuron 24, 187–203.

Grill-Spector, K., Kushnir, T., Hendler, T., Malach, R., 2000. The dynamics of object-selective activation correlate with recognition performance in humans. Nat. Neurosci. 3, 837–843.

Grill-Spector, K., Henson, R., Martin, A., 2006. Repetition and the brain: neural models of stimulus-specific effects. Trends Cogn. Sci. 10, 14–23.

Halgren, E., Dale, A.M., Sereno, M.I., Tootell, R.B.H., Marinkovic, K., Rosen, B.R., 1999. Location of human face-selective cortex with respect to retinotopic areas. Hum. Brain Mapp. 7, 29–37.

Hasson, U., Hendler, T., Ben Bashat, D., Malach, R., 2001. Vase or face? A neural correlate of shape-selective grouping processes in the human brain. J. Cogn. Neurosci. 13, 744–753.

Hasson, U., Harel, M., Levy, I., Malach, R., 2003. Large-scale mirror-symmetry organization of human occipito-temporal object areas. Neuron 37, 1027–1041.

Haxby, J.V., Gobbini, M.I., Furey, M.L., Ishai, A., Schouten, J.L., Pietrini, P., 2001. Distributed and overlapping representations of faces and objects in ventral temporal cortex. Science 293, 2425–2430.

Hon, N., Epstein, R.A., Owen, A.M., Duncan, J., 2006. Fronto-parietal activity with minimal decision and control. J. Neurosci. 26, 9805–9809.

Huk, A.C., Ress, D., Heeger, D.J., 2001. Neuronal basis of the motion aftereffect reconsidered. Neuron 32, 161–172.

Husain, M., Nachev, P., 2007. Space and the parietal cortex. Trends Cogn. Sci. 11, 30–36.

Ishai, A., Ungerleider, L.G., Martin, A., Schouten, H.L., Haxby, J.V., 1999. Distributed representation of objects in the human ventral visual pathway. Proc. Natl. Acad. Sci. U. S. A. 96, 9379–9384.

James, W., 1890. The Principles of Psychology. Henry Holt and Company, New York.

Kanwisher, N., McDermott, J., Chun, M.M., 1997. The fusiform face area: a module in human extrastriate cortex specialized for face perception. J. Neurosci. 17, 4302–4311.

Kastner, S., Ungerleider, L.G., 2000. Mechanisms of visual attention in the human cortex. Annu. Rev. Neurosci. 23, 315–341.

Klein, D., Zatorre, R.J., Chen, J.K., Milner, B., Crane, J., Belin, P., Bouffard, M., 2006. Bilingual brain organization: a functional magnetic resonance adaptation study. NeuroImage 31, 366–375.

Kourtzi, Z., Kanwisher, N., 2001. Representation of perceived object shape by the human lateral occipital complex. Science 293, 1506–1509.

Krekelberg, B., Vatakis, A., Kourtzi, Z., 2005. Implied motion from form in the human visual cortex. J. Neurophysiol. 94, 4373–4386.

Krekelberg, B., Boynton, G.M., van Wezel, R.J., 2006. Adaptation: from single cells to BOLD signals. Trends Neurosci. 29, 250–256.

Larsson, J., Heeger, D.J., 2006. Two retinotopic visual areas in human lateral occipital cortex. J. Neurosci. 26, 13128–13142.

Lerner, Y., Hendler, T., Malach, R., 2002. Object-completion effects in the human lateral occipital complex. Cereb. Cortex 12, 163–177.

Levy, I., Hasson, U., Avidan, G., Hendler, T., Malach, R., 2001. Center–periphery organization of human object areas. Nat. Neurosci. 4, 533–539.

Levy, I., Hasson, U., Harel, M., Malach, R., 2004. Functional analysis of the periphery effect in human building related areas. Hum. Brain Mapp. 22, 15–26.

Li Hegner, Y., Saur, R., Veit, R., Butts, R., Leiberg, S., Grodd, W., Braun, C., 2007. BOLD adaptation in vibrotactile stimulation: neuronal networks involved in frequency discrimination. J. Neurophysiol. 97, 264–271.

Lumer, E.D., Friston, K.J., Rees, G., 1998. Neural correlates of perceptual rivalry in the human brain. Science 280, 1930–1934.

Malach, R., Reppas, J.B., Benson, R.R., Kwong, K.K., Jiang, H., Kennedy, W.A., Ledden, P.J., Brady, T.J., Rosen, B.R., Tootell, R.B., 1995. Object-related activity revealed by functional magnetic resonance imaging in human occipital cortex. Proc. Natl. Acad. Sci. U. S. A. 92, 8135–8139.

Malach, R., Levy, I., Hasson, U., 2002. The topography of high-order human object areas. Trends Cogn. Sci. 6, 176–184.

McCarthy, G., Puce, A., Gore, J.C., Allison, T., 1997. Face specific processing in the human fusiform gyrus. J. Cogn. Neurosci. 9, 605–610.

McKyton, A., Zohary, E., 2007. Beyond retinotopic mapping: the spatial representation of objects in the human lateral occipital complex. Cereb. Cortex 17, 1164–1172.

Mesulam, M.M., 1999. Spatial attention and neglect: parietal, frontal and cingulate contributions to the mental representation and attentional targeting of salient extrapersonal events. Philos. Trans. R. Soc. Lond., B Biol. Sci. 354, 1325–1346.

Murray, S.O., Wojciulik, E., 2004. Attention increases neural selectivity in the human lateral occipital complex. Nat. Neurosci. 7, 70–74.

Pins, D., Ffytche, D., 2003. The neural correlates of conscious vision. Cereb. Cortex 13, 461–474.

Portas, C.M., Strange, B.A., Friston, K.J., Dolan, R.J., Frith, C.D., 2000. How does the brain sustain a visual percept? Proc. Biol. Sci. 267, 845–850.

Puce, A., Allison, T., Asgari, M., Gore, J.C., McCarthy, G., 1996. Differential sensitivity of human visual cortex to faces, letterstrings, and textures: a functional magnetic resonance imaging study. J. Neurosci. 16, 5205–5215.

Rees, G., Kreiman, G., Koch, C., 2002. Neural correlates of consciousness in humans. Nat. Rev., Neurosci. 3, 261–270.

Sala, J.B., Rama, P., Courtney, S.M., 2003. Functional topography of a distributed neural system for spatial and nonspatial information maintenance in working memory. Neuropsychologia 41, 341–356.

Sawamura, H., Georgieva, S., Vogels, R., Vanduffel, W., Orban, G.A., 2005. Using functional magnetic resonance imaging to assess adaptation and size invariance of shape processing by humans and monkeys. J. Neurosci. 25, 4294–4306.

Schiltz, C., Rossion, B., 2006. Faces are represented holistically in the human occipito-temporal cortex. NeuroImage 32, 1385–1394.

Sereno, M.I., McDonald, C.T., Allman, J.M., 1994. Analysis of retinotopic maps in extrastriate cortex. Cereb. Cortex 4, 601–620.

Shmuelof, L., Zohary, E., 2005. Dissociation between ventral and dorsal fMRI activation during object and action recognition. Neuron 47, 457–470.

Talairach, J., Tournoux, P., 1988. Co-Planar Stereotaxic Atlas of the Human Brain. Thieme Medical Publishers, New York.

Tong, F., Nakayama, K., Vaughan, K., Kanwisher, N., 1998. Binocular rivalry and visual awareness in human extrastriate cortex. Neuron 21, 753–759.

Tong, F., Nakayama, K., Moscovitch, M., Weinrib, O., Kanwisher, N., 2000. Response properties of the human fusiform face area. Cogn. Neuropsychol. 17, 257–279.

Tootell, R.B., Hadjikhani, N.K., Vanduffel, W., Liu, A.K., Mendola, J.D., Sereno, M.I., Dale, A.M., 1998. Functional analysis of primary visual cortex (V1) in humans. Proc. Natl. Acad. Sci. U. S. A. 95, 811–817.

Ullman, S., Vidal-Naquet, M., Sali, E., 2002. Visual features of intermediate complexity and their use in classification. Nat. Neurosci. 5, 682–687.

van Turennout, M., Ellmore, T., Martin, A., 2000. Long-lasting cortical plasticity in the object naming system. Nat. Neurosci. 3, 1329–1334.

van Turennout, M., Bielamowicz, L., Martin, A., 2003. Modulation of neural activity during object naming: effects of time and practice. Cereb. Cortex 13, 381–391.

Vuilleumier, P., Schwartz, S., Duhoux, S., Dolan, R.J., Driver, J., 2005. Selective attention modulates neural substrates of repetition priming and "implicit" visual memory: suppressions and enhancements revealed by FMRI. J. Cogn. Neurosci. 17, 1245–1260.

Wojciulik, E., Kanwisher, N., 1999. The generality of parietal involvement in visual attention. Neuron 23, 747–764.

Yi, D.J., Kelley, T.A., Marois, R., Chun, M.M., 2006. Attentional modulation of repetition attenuation is anatomically dissociable for scenes and faces. Brain Res. 1080, 53–62.